

Effect of Umklapp Scattering on Magnetic Field Penetration Depth in High- T_c Cuprates

Takanobu JUJO*

Department of Physics, Kyoto University, Kyoto 606-8502

(Received May 14, 2001)

The renormalization of the magnetic field penetration depth λ owing to the electron-electron correlation is discussed with its application to high- T_c cuprates. The formula for the current carried by quasiparticle with the Umklapp scattering is derived, on the basis of which we investigate how the value of λ^{-2} deviates from that of n/m^* where n and m^* are the carrier density and the effective mass respectively. Although this deviation is small in the case of weak momentum dependence of the vertex, this is large and negative owing to the non-negligible value of the backflow in the case of the strong antiferromagnetic spin fluctuation. The observed doping dependence of λ^{-2} in high- T_c cuprates, specifically a peak structure at the slightly overdoped region, is explained by the analytical consideration and the numerical calculation based on the perturbation theory and the spin fluctuation theory. The consistency between λ^{-2} and $d\lambda^{-2}/dT$ at absolute zero, which is the problem the isotropic model fails to explain, is also obtained by our theory.

KEYWORDS: Fermi liquid theory, high- T_c cuprates, current of quasiparticles, Umklapp scattering, electron-electron correlation, vertex correction, magnetic field penetration depth, perturbation theory, antiferromagnetic spin fluctuation

§1. Introduction

In high- T_c cuprates some transport phenomena show characteristic behaviors, especially in the optimal and the underdoped regions which do not seem to be explained by the conventional Fermi liquid theory. For examples, the resistivity is proportional to the temperature T , rather than T^2 .¹⁾ The Hall coefficient is temperature dependent and increases as the doping level decreases.²⁾ It is also seen that not only these transport phenomena, but also the magnetic properties like the nuclear spin-lattice relaxation rate and the one-particle spectrum show the pseudo gap phenomenon which is the gap like behavior with no long range order. The magnetic field penetration depth λ in the high- T_c cuprates attracts attention because λ is long in the underdoped region where the

* E-mail: jujo@ton.scphys.kyoto-u.ac.jp

pseudogap phenomena appear and then some authors suggest the low carrier density based on the relation $\lambda^{-2} \propto n/m^*$ where n, m^* are the carrier density and the effective mass, respectively,³⁾ and a connection between long λ and the pseudogap phenomena.⁴⁾

In the above phenomena it is found in the early stage of the study on the high- T_c cuprates that the T -linear resistivity is explained by the fact that the lifetime of the quasiparticles is proportional to T in the presence of the strong antiferromagnetic spin fluctuation.^{5),6)} This means that it is sufficient to consider an one-particle property like the imaginary part of the self-energy. The pseudo gap phenomena can also be explained by the superconducting fluctuation with the two dimensional and the strong coupling nature of the system.^{7),8)} In this case the absolute value of the imaginary part of the self-energy shows the maximum at the Fermi level and therefore one particle spectrum decreases. On the other hand it is found that the interaction between the quasiparticles is essential for the explanation of the Hall coefficient.⁹⁾ This work clarifies the importance of the interaction between the quasiparticles besides one-particle properties like the self-energy.

As for the magnetic field penetration depth in high- T_c cuprates, there has been no satisfactory theories until now. As noted above it seems that λ^{-2} is proportional to the doping concentration δ , and from the combination with $\lambda^{-2} \propto n/m^*$ it seems to be reasonable to expect that the effective carrier density is identified with the doping concentration (i.e. $n \propto \delta$).³⁾ The theories based on the t - J model naturally accept this conjecture because of no double occupation. There is no need to explain why λ^{-2} is so small but it needs only to take it as an external parameter in these theories.¹⁰⁾ However the doping dependences of λ^{-2} show that λ^{-2} increases with δ in the underdoped and optimal regions, and it has a peak at the slightly overdoped region, and then it decreases as δ increases in the overdoped region.¹¹⁾ It is obvious that the latter behavior cannot be explained by the theory based on the t - J model. On the other hand n should be proportional to $1 - \delta$ in the Fermi gas theory because $\delta = 0$ means the half-filled, and therefore based on $\lambda^{-2} \propto n/m^*$ it can explain the overdoped region but cannot explain the optimal and underdoped regions. If we take account of the interaction between the quasiparticles, it is known that $\lambda^{-2} \propto n(1 + F_1^s/3)/m^*$.¹²⁾ Here F_1^s is one of the Landau parameters and this expression is based on the isotropic model. Though the behavior of this parameter is not known, it is seemingly possible to explain the doping dependence of λ^{-2} by controlling the parameter F_1^s . However it is shown that this parameter theory fails if we try to maintain the consistency between the values of λ^{-2} and $d\lambda^{-2}/dT$ at absolute zero.¹³⁾ These considerations indicate that the isotropic formalism presented by Leggett should be reexamined to investigate the realistic metallic system like the high- T_c cuprates, and it cannot be permitted to take F_1^s as an external parameter either, necessitating the investigation of the quantities corresponding to F_1^s in detail.

The Umklapp scattering, a main interest in this paper, is important for the transport phenomena. In the previous paper a systematic discussion on how the many body effect appears in the

superconducting state, is presented.¹⁴⁾ Some examples presented there, are the magnetic field penetration depth and the optical conductivity. At absolute zero the expression of the magnetic field penetration depth contains the interaction between quasiparticles in the same way as in the cyclotron resonance frequency¹⁵⁾ and the Drude weight.^{16),17)} In ref.18 it is shown that the absence of the Umklapp scattering leads to the infinite conductivity. Although this fact can be shown by using the Ward-Takahashi identity related with the momentum conservation, the essential point in ref.18 is that the formula for the resistivity is written explicitly by the Umklapp process. The formula for the current which is explicitly written by the Umklapp scattering has not been known. The derivation of this formula is given in this paper. With regard to high- T_c cuprates it is needed to clarify the relation between the Umklapp scattering and the antiferromagnetic spin fluctuation and it is shown that the strong antiferromagnetic spin fluctuation leads to the strong Umklapp scattering on the current.

In §2 the formula for the current carried by quasiparticles written by the Umklapp scattering is derived and the other property of the current is briefly discussed. In §3 the model and the approximations for the analytical and the numerical calculations are presented. Some discussions on the influence of the superconducting transition is also given and the validity of the calculation of the current in the normal state is shown. In §4 the analytical investigation for the current is presented in the two specific cases. One is the case where the momentum dependence of the irreducible four point vertex is weak and the other is the case with the strong antiferromagnetic spin fluctuation. It is shown that the discussions based on $\lambda^{-2} \propto n/m^*$ is approximately valid only in the former case. In the latter case the behaviors of the current differ with the others depending on the points on the Fermi surface and it is shown that the current on the points with the strong antiferromagnetic spin fluctuation is decreased much. How the effect of the Umklapp scattering on the current depends on the irreducible four point vertex is also presented and it is shown that it is largest in the case of the strong antiferromagnetic spin fluctuation and is smallest in the case of the ferromagnetic spin fluctuation. It is also presented that the backflow in the case of the strong antiferromagnetic spin fluctuation has an opposite sign to the bare velocity. In §5 the numerical calculations with the self-consistent second order perturbation theory (SC-SOPT) and the fluctuation exchange approximation (FLEX) are presented. The results which are consistent with the experiments in the respects of the doping dependence of λ^{-2} at absolute zero and the consistency between λ^{-2} and $d\lambda^{-2}/dT$, are obtained. In §6 a brief consideration on the relation between the superconducting fluctuation and λ^{-2} is given and it is indicated that the small λ^{-2} at absolute zero does not directly mean the large thermal fluctuation. In §7 the summary and the discussion are given.

In this paper we put $\hbar = k_B = c = 1$.

§2. Current Carried by Quasiparticles

The current carried by quasiparticles plays an important role in physical quantities of the collisionless region in the normal state, for example, the cyclotron resonance frequency and the Drude weight. This is usually written by using only quantities defined on the Fermi surface as

$$j_{\mathbf{k}\mu}^* = v_{\mathbf{k}\mu}^* + \frac{1}{V} \sum_{\mathbf{k}} f_{\mathbf{k},\mathbf{k}'} \delta(\xi_{\mathbf{k}'}^*) v_{\mathbf{k}'\mu}^*. \quad (2.1)$$

Here μ is the index of spatial dimensions, V is the volume of the system, $\xi_{\mathbf{k}}^*$ is the dispersion of the quasiparticles including the chemical potential, $v_{\mathbf{k}\mu}^*$ is the renormalized velocity of quasiparticles ($v_{\mathbf{k}}^* = \frac{\partial \xi_{\mathbf{k}}^*}{\partial \mathbf{k}}$) and $f_{\mathbf{k},\mathbf{k}'} = z_{\mathbf{k}} \Gamma_{\mathbf{k},\mathbf{k}'}^\omega z_{\mathbf{k}'}$ is the interaction between quasiparticles (Γ^ω is the ω -limit of reducible four-point vertex and the notation about ω -limit and k -limit is the same as in ref.19). In the superconducting state the magnetic field penetration depth is also written by using this quantity at absolute zero. As derived in the previous paper,¹⁴⁾ the magnetic field penetration depth λ at finite temperature is written as

$$\left(\frac{1}{\lambda^2}\right)_{\mu\nu} \propto \int_{\text{FS}} \frac{dS_{\mathbf{k}}}{4\pi^3 |v^*(\mathbf{k})|} v_{\mu}^*(\mathbf{k}) (1 - Y(\mathbf{k}; T)) \bar{v}_{\nu}^*(\mathbf{k}; T). \quad (2.2)$$

Here $\int_{\text{FS}} dS_{\mathbf{k}}$ is the integral over the Fermi surface and $Y(\mathbf{k}; T)$ is Yosida function

$$Y(\mathbf{k}; T) = \int d\xi_{\mathbf{k}}^* \left(-\frac{\partial f(E_{\mathbf{k}}^*)}{\partial E_{\mathbf{k}}^*} \right), \quad (2.3)$$

$f(x) := 1/(e^{x/T} + 1)$, $E_{\mathbf{k}}^* = \sqrt{(\xi_{\mathbf{k}}^{*2} + \Delta_{\mathbf{k}}^2)}$, $\Delta_{\mathbf{k}}$ is the superconducting gap and $\bar{v}_{\nu}^*(\mathbf{k}; T)$ satisfies the following integral equation,

$$\bar{v}_{\nu}^*(\mathbf{k}; T) = j_{\nu}^*(\mathbf{k}) - \int_{\text{FS}} \frac{dS_{\mathbf{k}'}}{4\pi^3 |v^*(\mathbf{k}')|} f_{\mathbf{k},\mathbf{k}'} Y(\mathbf{k}'; T) \bar{v}_{\nu}^*(\mathbf{k}'; T), \quad (2.4)$$

or

$$\bar{v}_{\nu}^*(\mathbf{k}; T) = v_{\nu}^*(\mathbf{k}) + \int_{\text{FS}} \frac{dS_{\mathbf{k}'}}{4\pi^3 |v^*(\mathbf{k}')|} A_{\mathbf{k},\mathbf{k}'} (1 - Y(\mathbf{k}'; T)) \bar{v}_{\nu}^*(\mathbf{k}'; T). \quad (2.5)$$

Then it can be seen that $\bar{v}_{\nu}^*(\mathbf{k}; T) = j_{\nu}^*(\mathbf{k})$ at absolute zero because of $Y(\mathbf{k}; T=0) = 0$. Here $A_{\mathbf{k},\mathbf{k}'} = z_{\mathbf{k}} \Gamma_{\mathbf{k},\mathbf{k}'}^k z_{\mathbf{k}'}$ ($\Gamma_{\mathbf{k},\mathbf{k}'}^k$ is the k -limit of the reducible four point vertex) and this satisfies the following equation:

$$f_{\mathbf{k},\mathbf{k}'} = A_{\mathbf{k},\mathbf{k}'} + \frac{1}{V} \sum_{\mathbf{k}''} A_{\mathbf{k},\mathbf{k}''} \left(-\frac{\partial f(\xi_{\mathbf{k}''}^*)}{\partial \xi_{\mathbf{k}''}^*} \right) f_{\mathbf{k}'',\mathbf{k}'}. \quad (2.6)$$

Here we briefly explain why λ^{-2} is not generally written as n/m^* , and how the many body effect enters. The electromagnetic response kernel is written as

$$K_{\mu\nu} = - \int_{\mathbf{k}} v_{\mathbf{k}\mu} (GG + FF)_{\mathbf{k}}(\epsilon) \Lambda_{\mathbf{k}\nu}(\epsilon) - \left(\frac{n}{m}\right)_{\mu\nu}. \quad (2.7)$$

Here G and F are the normal and the anomalous Green's function, respectively, in the superconducting state in the usual sense,¹⁹⁾ m is the bare mass, $v_{\mathbf{k}\mu}$ is the bare velocity and $\Lambda_{\mathbf{k}\nu}(\epsilon)$ is the three

point vertex which satisfies the integral equation with the interaction included. $\int_k := \int \frac{d\epsilon}{4\pi iV} \sum_{\mathbf{k}}$ is used in the zero temperature formalism hereafter. In the case of the finite temperature formalism $\int_k := \int \frac{d\epsilon}{2\pi V} \sum_{\mathbf{k}}$ is used. The first term of the r.h.s. of eq.(2.7) is often called paramagnetic term and the second term is called diamagnetic term. In the usual textbook²⁰⁾ it is explained that the paramagnetic term vanishes at absolute zero in the superconducting state. This is valid in the case where the superconducting gap grows in the whole Fermi sea and then the integral which includes $GG+FF$ reduced to Yosida function and vanishes at absolute zero. However in all superconductors the superconducting gap grows only near the Fermi surface and the incoherent part contributes to the integral which does not vanish in the lattice system. Then the eq.(2.7) is reduced to the following equation at absolute zero, instead of to $-n/m$.

$$K_{\mu\nu} = - \int_k v_{\mathbf{k}\mu} (GG)_{\mathbf{k}}^{\text{inc}}(\epsilon) \Lambda_{\mathbf{k}\nu}(\epsilon) - \left(\frac{n}{m}\right)_{\mu\nu}. \quad (2.8)$$

In the same way $\Lambda_{\mathbf{k}\nu}(\epsilon)$ satisfies the following integral equation.

$$\Lambda_{\mathbf{k}\nu}(\epsilon) = v_{\mathbf{k}\nu} + \int_{k'} I_{\mathbf{k},\mathbf{k}'}(\epsilon, \epsilon') (GG)_{\mathbf{k}'}^{\text{inc}}(\epsilon') \Lambda_{\mathbf{k}'\nu}(\epsilon'). \quad (2.9)$$

($I_{\mathbf{k},\mathbf{k}'}(\epsilon, \epsilon')$ is the irreducible four-point vertex.) Then from eqs.(2.7) and (2.9) the formalism of magnetic field penetration depth based on Fermi liquid theory is derived by integrating the high energy part to derive the low energy dynamics as investigated in detail in ref.14. In the specific case where the momentum is conserved it can be shown that the paramagnetic term exactly vanishes at absolute zero as follows. In this case Ward-Takahashi identity which reflect the momentum conservation is written as

$$\Lambda_{\mathbf{k}\nu}(\epsilon) = \left(1 - \frac{\partial \Sigma_{\mathbf{k}}^n(\epsilon)}{\partial \epsilon}\right) v_{\mathbf{k}\nu}. \quad (2.10)$$

($\Sigma_{\mathbf{k}}^n(\epsilon)$ is the normal self-energy.) This relation holds at arbitrary value of ϵ . Then the paramagnetic term is

$$- \int_k v_{\mathbf{k}\mu} (GG)_{\mathbf{k}}^{\text{inc}}(\epsilon) \left(1 - \frac{\partial \Sigma_{\mathbf{k}}^n(\epsilon)}{\partial \epsilon}\right) v_{\mathbf{k}\nu} = \int_k v_{\mathbf{k}\mu} v_{\mathbf{k}\nu} \frac{\partial G_{\mathbf{k}}(\epsilon)}{\partial \epsilon} \quad (2.11)$$

$$= 0. \quad (2.12)$$

This is the direct proof of the disappearance of the paramagnetic term in the case where the momentum conservation holds, which is not via the Fermi liquid parameter like F_1^s .

Next we discuss the role of the Umklapp scattering. Hereafter in this section the discussion is given by using the Green's function in the normal state. In the superconducting state equations become more complicated, but the main results are not altered as partly discussed in ref.14 about the renormalization factor and the renormalized velocity and in §3.1. By using the fact that the renormalized velocity and the renormalization factor is written as (k is a simplified notation of (\mathbf{k}, ϵ) in the zero temperature formalism),

$$v_{\mathbf{k}\mu}^* = z_{\mathbf{k}} (v_{\mathbf{k}\mu} + \int_{k'} \Gamma_{\mathbf{k},\mathbf{k}'}^k(0, \epsilon') [G(k')]^2 v_{\mathbf{k}'\mu}) \quad (2.13)$$

and

$$z_{\mathbf{k}}^{-1} = 1 + \int_{k'} \Gamma_{\mathbf{k}, \mathbf{k}'}^{\omega}(0, \epsilon') [G(k')]^{2\omega} \quad (2.14)$$

respectively, and also noting that

$$[G(k)]^{2\omega} - [G(k)]^{2k} = 2\pi i \delta(\epsilon) \delta(\xi_{\mathbf{k}}^*), \quad (2.15)$$

eq.(2.1) is written as

$$j_{\mathbf{k}\mu}^* = v_{\mathbf{k}\mu} + z_{\mathbf{k}} \int_{k'} \Gamma_{\mathbf{k}, \mathbf{k}'}^{\omega}(0, \epsilon') [G(k')]^{2\omega} (v_{\mathbf{k}'\mu} - v_{\mathbf{k}\mu}), \quad (2.16)$$

or

$$j_{\mathbf{k}\mu}^* = v_{\mathbf{k}\mu} + z_{\mathbf{k}} \left(\frac{d\Sigma(k)}{d\mathbf{k}} + \frac{\partial\Sigma(k)}{\partial\epsilon} v_{\mathbf{k}\mu} \right)_{\epsilon=0}. \quad (2.17)$$

Here $\frac{d\Sigma(k)}{d\mathbf{k}}$ is the same notation as in ref.21 and it means the derivative with the Fermi surface also transformed, in the contrary to $\frac{\partial\Sigma(k)}{\partial\mathbf{k}}$, the derivative with the Fermi surface fixed. Reflecting the simultaneous transformation of the Fermi surface, $\frac{d\Sigma(k)}{d\mathbf{k}}$ corresponds to the ω -limit, and $\frac{\partial\Sigma(k)}{\partial\mathbf{k}}$ to the k -limit owing to the inclusion of the discontinuity on the Fermi surface.

The quantities, $\frac{d\Sigma(k)}{d\mathbf{k}}$ and $\frac{\partial\Sigma(k)}{\partial\epsilon}$, satisfy the following integral equations, respectively.

$$\frac{d\Sigma(k)}{d\mathbf{k}} = \int_{k'} I(k, k') [G(k')]^{2\omega} \left(\mathbf{v}_{\mathbf{k}'} + \frac{d\Sigma(k')}{d\mathbf{k}'} \right) \quad (2.18)$$

and

$$\frac{\partial\Sigma(k)}{\partial\epsilon} = - \int_{k'} I(k, k') [G(k')]^{2\omega} \left(1 - \frac{\partial\Sigma(k')}{\partial\epsilon'} \right). \quad (2.19)$$

Then it is verified that $\mathbf{w}_{\mathbf{k}}(\epsilon) := \frac{d\Sigma(k)}{d\mathbf{k}} + \frac{\partial\Sigma(k)}{\partial\epsilon} \mathbf{v}_{\mathbf{k}}$ satisfies the following integral equation.

$$\mathbf{w}_{\mathbf{k}}(\epsilon) = \mathbf{u}_{\mathbf{k}}(\epsilon) + \int_{k'} I(k, k') [G(k')]^{2\omega} \mathbf{w}_{\mathbf{k}'}(\epsilon') \quad (2.20)$$

$$= \mathbf{u}_{\mathbf{k}}(\epsilon) + \int_{k'} \Gamma^{\omega}(k, k') [G(k')]^{2\omega} \mathbf{u}_{\mathbf{k}'}(\epsilon'). \quad (2.21)$$

Here

$$\mathbf{u}_{\mathbf{k}\mu}(\epsilon) = \int_{k'} I(k, k') [G(k')]^{2\omega} \left(1 - \frac{\partial\Sigma(k')}{\partial\epsilon'} \right) (v_{\mathbf{k}'\mu} - v_{\mathbf{k}\mu}). \quad (2.22)$$

This is rewritten as

$$\mathbf{u}_{\mathbf{k}}(\epsilon) = \int_{k'} I(k, k') \left(-\frac{\partial G(k')}{\partial\epsilon'} \right) \mathbf{v}_{\mathbf{k}'} + \frac{\partial\Sigma(k)}{\partial\epsilon} \mathbf{v}_{\mathbf{k}} \quad (2.23)$$

$$= \int_{k'} \int_q |\Gamma(k, k'; q)|^2 G(k-q) G(k'+q) \left(-\frac{\partial G(k')}{\partial\epsilon'} \right) (\mathbf{v}_{\mathbf{k}'+\mathbf{q}} + \mathbf{v}_{\mathbf{k}-\mathbf{q}} - \mathbf{v}_{\mathbf{k}'} - \mathbf{v}_{\mathbf{k}}). \quad (2.24)$$

This equation shows that $\mathbf{u}_{\mathbf{k}}(\epsilon) = \mathbf{o}$ in the absence of the Umklapp process and the concrete examples are given in §3 in the case of SC-SOPT and FLEX approximations. By using the above quantities the backflow term is written by the difference between the two kinds of the momentum derivative of self-energy.

$$\frac{d\Sigma(k)}{d\mathbf{k}} - \frac{\partial\Sigma(k)}{\partial\mathbf{k}} = \frac{\mathbf{B}_{\mathbf{k}}}{z_{\mathbf{k}}}. \quad (2.25)$$

Here $B_{\mathbf{k}}$ is the backflow term.

In ref.15 $j_{\mathbf{k}\mu}^*$ is calculated based on second order perturbation theory with respect to the on-site Coulomb interaction. It is mentioned there that the four-point interaction vertex is taken to satisfy the conservation law and they obtained the results that the vertex correction make the positive value in some parameter regions. If this holds, it follows that the value of current carried by quasiparticles exceeds the value of the bare electron's velocity. However it is not considered to be possible for the interacting electrons to carry the current which exceeds the non-interacting case because if it were possible, gathering the momentum from the crystalline lattice and carrying it would occur. If we see the general expressions above it is obvious that their treatment is incorrect. To satisfy the conservation law and get the correct value of $j_{\mathbf{k}\mu}^*$, it is needed to use eq.(2.24) as the vertex correction with $|\Gamma(k, k'; q)|^2$ replaced by U^2 in the case of the second order perturbation. The fact that $j_{\mathbf{k}\mu}^*$ does not exceeds $v_{\mathbf{k}\mu}$ is made clear by eq.(2.16) with the notion that $v_{\mathbf{k}\mu}$ is an odd function with respect to \mathbf{k} and $\int_{k'} \Gamma_{\mathbf{k}, \mathbf{k}'}^\omega(0, \epsilon') [G(k')^2]^\omega > 0$ in the Fermi liquid system. Then $j_{\mathbf{k}\mu}^* < v_{\mathbf{k}\mu}$ in \mathbf{k} with $v_{\mathbf{k}\mu} > 0$, and this is the basic inequality which can be obtained from the above general discussion. This inequality also guarantee that λ^{-2} is always smaller than $4\pi e^2 n/m$.

By taking the above results into account we consider how the currents j^* in the lattice system changes from the value $j^* = v$ which is universal in the case of the continuum. If we consider this correction in terms of the renormalization factor (z), it can be seen that this quantity is changes as $(1 - z^{-1})/z^{-1}$ plus the extra contribution proportional to z which depends on the system considered. The presence of this extra contribution violates the relation $\lambda \propto n/m^*$ and expresses one of the characteristics of the system like the momentum dependence of the interaction between the quasiparticles. This property in high- T_c cuprates is investigated in detail in §4 and 5.

§3. Model and Approximation

We take the following Hubbard Hamiltonian with on-site Coulomb interaction.

$$\mathcal{H} = \sum_{\mathbf{k}, \sigma} \xi_{\mathbf{k}} c_{\mathbf{k}\sigma}^\dagger c_{\mathbf{k}\sigma} + U \sum_{\mathbf{k}, \mathbf{k}', \mathbf{q}} c_{\mathbf{k}+\mathbf{q}\uparrow}^\dagger c_{\mathbf{k}'-\mathbf{q}\downarrow}^\dagger c_{\mathbf{k}'\downarrow} c_{\mathbf{k}\uparrow}. \quad (3.1)$$

Here $\xi_{\mathbf{k}}$ is the dispersion of electrons which is taken similar to that in ref.9.

$$\xi_{\mathbf{k}} = -2t(\cos k_x + \cos k_y) + 4t' \cos k_x \cos k_y - 2t''(\cos 2k_x + \cos 2k_y). \quad (3.2)$$

In the numerical calculation we put $t'/t = 0.16$, $t''/t = 0.20$, $U/t = 7.0$ and $t = 1$.

The self-energy within SC-SOPT is

$$\Sigma(k) = \frac{T}{V} \sum_q \chi(q) G(k - q). \quad (3.3)$$

Here $k = (\mathbf{k}, i\epsilon_n)$ (ϵ_n is the Matsubara frequency),

$$G(k) = \frac{1}{i\epsilon_n - \xi_{\mathbf{k}} - \Sigma(k)} \quad (3.4)$$

and

$$\chi(q) = -\frac{T}{V} \sum_{k'} G(k')G(k' + q). \quad (3.5)$$

The irreducible four point vertex is

$$\begin{aligned} I(k, k') &= \frac{\delta\Sigma(k)}{\delta G(k')} \\ &= 2\chi(k - k') + \phi(k + k'). \end{aligned} \quad (3.6)$$

The first line of this equation follows the conserving approximation by Baym and Kadanoff.²²⁾ Here

$$\phi(q) = -\frac{T}{V} \sum_{k'} G(k')G(q - k'). \quad (3.7)$$

$\Gamma_{\mathbf{k}, \mathbf{k}'}^{(a)}(\epsilon, \epsilon')$ and $\Gamma_{\mathbf{k}, \mathbf{k}'}^{(b)}(\epsilon, \epsilon')$ in the basic formalism in Appendix are given by the following expressions.

$$\Gamma_{\mathbf{k}, \mathbf{k}'}^{(a)}(\epsilon, \epsilon') = 2\chi_{\mathbf{k}-\mathbf{k}'}^R(\epsilon - \epsilon') \quad (3.8)$$

and

$$\Gamma_{\mathbf{k}, \mathbf{k}'}^{(b)}(\epsilon, \epsilon') = \phi_{\mathbf{k}+\mathbf{k}'}^R(\epsilon + \epsilon'). \quad (3.9)$$

By using the above $I(k, k')$, $\mathbf{u}_{\mathbf{k}}(\epsilon)$ which expresses the Umklapp term is explicitly written as

$$\mathbf{u}_{\mathbf{k}}(\epsilon) = U^2 \int_{k'} \int_q G_{\mathbf{k}-\mathbf{q}}(\epsilon - \omega) G_{\mathbf{k}'+\mathbf{q}}(\epsilon' + \omega) \frac{\partial G_{\mathbf{k}'}(\epsilon')}{\partial \epsilon'} (\mathbf{v}_{\mathbf{k}} + \mathbf{v}_{\mathbf{k}'} - \mathbf{v}_{\mathbf{k}'+\mathbf{q}} - \mathbf{v}_{\mathbf{k}-\mathbf{q}}) \quad (3.10)$$

As can be easily seen by explicit calculation $-\mathbf{v}_{\mathbf{k}-\mathbf{q}}$ term and $-\mathbf{v}_{\mathbf{k}'+\mathbf{q}}$ in the above equation originate from $2\chi(q)$ term in $I(k, k')$, $\mathbf{v}_{\mathbf{k}'}$ term from $\phi(q)$ and $\mathbf{v}_{\mathbf{k}}$ term from $\partial\Sigma(k)/\partial\epsilon$.

The basic equations in the FLEX approximation are (for an example, see ref.23),

$$\Sigma(k) = \frac{T}{V} \sum_q V(q)G(k - q), \quad (3.11)$$

$$V(q) = \frac{3}{2}U^2 \frac{\chi(q)}{1 - U\chi(q)} + \frac{1}{2}U^2 \frac{\chi(q)}{1 + U\chi(q)} - U^2\chi(q). \quad (3.12)$$

The irreducible four-point vertex in this approximation is

$$\begin{aligned} I(k, k') &= \frac{\delta\Sigma(k)}{\delta G(k')} \\ &= V(k - k') - \frac{T}{V} \sum_q W(q)[G(k' - q)G(k - q) + G(k' + q)G(k - q)]. \end{aligned} \quad (3.13)$$

Here

$$W(q) = \frac{3}{2}U^2 \frac{1}{|1 - U\chi(q)|^2} + \frac{1}{2}U^2 \frac{1}{|1 + U\chi(q)|^2} - U^2. \quad (3.14)$$

$\Gamma_{\mathbf{k}, \mathbf{k}'}^{(a)}(\epsilon, \epsilon')$ and $\Gamma_{\mathbf{k}, \mathbf{k}'}^{(b)}(\epsilon, \epsilon')$ in the basic formalism in Appendix are given by the following expressions.

$$\begin{aligned} \Gamma_{\mathbf{k}, \mathbf{k}'}^{(a)}(\epsilon, \epsilon') &= V_{\mathbf{k}-\mathbf{k}'}^R(\epsilon - \epsilon') - \frac{1}{V} \sum_q \int \frac{d\omega}{2\pi} W_{\mathbf{q}}(\omega) [\tanh \frac{\epsilon - \omega}{2T} \text{Im} G_{\mathbf{k}-\mathbf{q}}^R(\epsilon - \omega) G_{\mathbf{k}'-\mathbf{q}}^A(\epsilon' - \omega) \\ &\quad + \tanh \frac{\epsilon' - \omega}{2T} G_{\mathbf{k}-\mathbf{q}}^R(\epsilon - \omega) \text{Im} G_{\mathbf{k}'-\mathbf{q}}^R(\epsilon' - \omega)] \end{aligned} \quad (3.15)$$

and

$$\begin{aligned} \Gamma_{\mathbf{k}, \mathbf{k}'}^{(b)}(\epsilon, \epsilon') &= -\frac{1}{V} \sum_{\mathbf{q}} \int \frac{d\omega}{2\pi} W_{\mathbf{q}}(\omega) \left[\tanh \frac{\epsilon - \omega}{2T} \text{Im} G_{\mathbf{k}-\mathbf{q}}^R(\epsilon - \omega) G_{\mathbf{k}'+\mathbf{q}}^R(\epsilon' + \omega) \right. \\ &\quad \left. + \tanh \frac{\epsilon' + \omega}{2T} G_{\mathbf{k}-\mathbf{q}}^R(\epsilon - \omega) \text{Im} G_{\mathbf{k}'+\mathbf{q}}^R(\epsilon' + \omega) \right]. \end{aligned} \quad (3.16)$$

By using the above $I(k, k')$, $\mathbf{u}_{\mathbf{k}}(\epsilon)$ which expresses the Umklapp term is explicitly written as

$$\mathbf{u}_{\mathbf{k}}(\epsilon) = \int_{k'} \int_{\mathbf{q}} W_{\mathbf{q}}(\omega) G_{\mathbf{k}-\mathbf{q}}(\epsilon - \omega) G_{\mathbf{k}'+\mathbf{q}}(\epsilon' + \omega) \frac{\partial G_{\mathbf{k}'}^R(\epsilon')}{\partial \epsilon'} (\mathbf{v}_{\mathbf{k}} + \mathbf{v}_{\mathbf{k}'} - \mathbf{v}_{\mathbf{k}'+\mathbf{q}} - \mathbf{v}_{\mathbf{k}-\mathbf{q}}) \quad (3.17)$$

As can be easily seen by explicit calculation $-\mathbf{v}_{\mathbf{k}-\mathbf{q}}$ term in the above equation originate from $V(q)$ term in $I(k, k')$, $-\mathbf{v}_{\mathbf{k}'+\mathbf{q}}$ term from the second term of r.h.s. of eq.(3.13), $\mathbf{v}_{\mathbf{k}'}$ term from the third term of r.h.s. of eq.(3.13) and $\mathbf{v}_{\mathbf{k}}$ term from $\partial \Sigma(k)/\partial \epsilon$.

By using the above approximations, it is shown that the momentum dependence of $V_{\mathbf{q}}^R(0)$ is remarkable at $\mathbf{q} = (\pi, \pi)$. On the other hand, although $\chi_{\mathbf{q}}^R(0)$ has a small peak around $\mathbf{q} = (\pi, \pi)$ and $\phi_{\mathbf{q}}^R(0)$ at $\mathbf{q} = (0, 0)$, it can be seen that the momentum dependence of the irreducible four point vertex in SC-SOPT is rather weak as compared with that in FLEX.

3.1 Influence of Superconducting Transition

Here we briefly discuss how the electronic properties differ between the normal state and the superconducting state, and take the renormalization factor and the damping rate of the quasiparticles as the representative quantities because the renormalization factor is related to the vertex corrections to the current by the real part of the irreducible four point vertex and the damping rate of the quasiparticles is related to the vertex correction in the hydrodynamic region by the imaginary part. It is known that the imaginary part of the vertex caused by the electron-electron interaction becomes small at the low energy in the superconducting state because of the decrease of the scattering accompanied by the gap formation, while the real part is not so affected at low energy except for the uniform magnetic susceptibility in the case of the singlet pairing.

The imaginary part of the self-energy and the renormalization factor calculated numerically in the FLEX approximation is shown in Fig. 1. From this figure it is shown that $-\text{Im} \Sigma_{\mathbf{k}}^R(0)$ rapidly decreases below T_c as expected from the above consideration. A notable point concerning the damping rate, which is not related to the present discussion, is that the damping rate at the cold spot decreases linearly with the temperature and that at the hot spot decreases as \sqrt{T} . The former point causes the T -linear resistivity and the latter point does not affect the conductivity because the point with the smallest damping rate mainly contributes to the conductivity.

On the other hand the renormalization factor almost remains constant as expected also, while the change in the spectrum of the spin fluctuation makes the minimum of this quantity at $T = T_c$. These considerations justify the calculation of the current in the normal state to estimate the

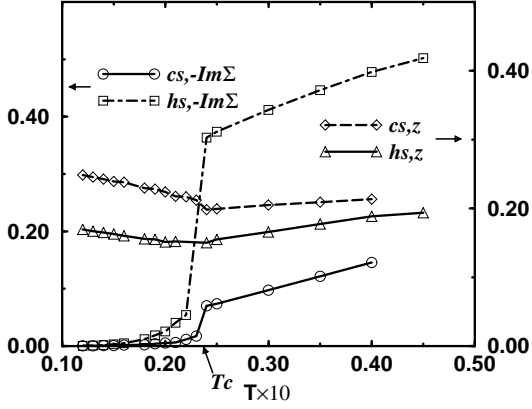


Fig. 1. $-\text{Im}\Sigma_{\mathbf{k}}^R(0)$ and the renormalization factor (z) at the cold spot (cs) and the hot spot (hs). $\delta = 0.10$ and $T_c = 0.024$.

magnetic field penetration depth because the vertex correction for the current is the type of the function analogous to the renormalization factor.

§4. Analysis of Umklapp Term

4.1 The case where the momentum dependence of $I_{\mathbf{k},\mathbf{k}'}$ is weak

This case occurs when the shape of the Fermi surface is not so peculiar and the perturbation scheme is valid. Then it is easy to derive the following relation by using the fact that the velocity is an odd function of \mathbf{k} .

$$\mathbf{w}_{\mathbf{k}}(\epsilon) \simeq \mathbf{u}_{\mathbf{k}}(\epsilon) \quad (4.1)$$

$$\simeq \int_{\mathbf{k}'} I_{\mathbf{k},\mathbf{k}'}(\epsilon, \epsilon') \frac{\partial G_{\mathbf{k}'}(\epsilon')}{\partial \epsilon'} \mathbf{v}_{\mathbf{k}} \quad (4.2)$$

$$= \frac{\partial \Sigma_{\mathbf{k}}(\epsilon)}{\partial \epsilon} \mathbf{v}_{\mathbf{k}}. \quad (4.3)$$

Then the current is written as

$$j_{\mathbf{k}\mu}^* \simeq v_{\mathbf{k}\mu} + z_{\mathbf{k}} \frac{\partial \Sigma_{\mathbf{k}}(\epsilon)}{\partial \epsilon} \Big|_{\epsilon=0} v_{\mathbf{k}\mu} \quad (4.4)$$

$$= z_{\mathbf{k}} v_{\mathbf{k}\mu} \quad (4.5)$$

This equation shows that the Umklapp term reduces to $(z_{\mathbf{k}} - 1)\mathbf{v}_{\mathbf{k}}$. The current and λ^{-2} is only reduced by $z_{\mathbf{k}}$ and then the latter quantity is interpreted by writing n/m^* as used *a priori* in the some papers,³⁾ where m^* is the thermal mass which is enhanced by $1/z$. However it is considered that in the case of high- T_c the validity of this perturbation scheme is restricted in the overdoped region. This assertion is understood by noting the behavior of the nuclear spin relaxation rate and

the resistivity measurements. Therefore the use of the form n/m^* in the underdoped cuprates, which is taken in some papers, is not warranted.

4.2 The case of strong antiferromagnetic spin fluctuation

This is the case which is relevant to the optimal and underdoped cuprates. In this case $W_{\mathbf{q}}(\omega)$ has a sharp peak at $\mathbf{q} \simeq \mathbf{Q}$ and $\omega \simeq 0$ ($\mathbf{Q} = (\pi, \pi)$). The fact that $W_{\mathbf{q}}$ takes a large value at a specific momentum reduces the integral including $W_{\mathbf{q}}$ to the one that is the integral of the odd function $v_{\mathbf{k}}$, and then the term including $W_{\mathbf{q}}$ can be neglected, as confirmed numerically. Then eqs.(2.20) and (2.22) (the corresponding equations in Appendix) is reduced to the following equations.

$$\mathbf{w}_{\mathbf{k}}^R(0) = \mathbf{u}_{\mathbf{k}}^R(0) + \int_{k'} [\coth \frac{\epsilon'}{2T} \text{Im} V_{\mathbf{k}-\mathbf{k}'}^R(-\epsilon') \frac{\partial \text{Re} G_{\mathbf{k}'}^R(\epsilon')}{\partial \epsilon'} + \tanh \frac{\epsilon'}{2T} \frac{\partial \text{Re} V_{\mathbf{k}-\mathbf{k}'}^R(-\epsilon')}{\partial \epsilon'} \text{Im} G_{\mathbf{k}'}^R(\epsilon')] z_{\mathbf{k}'} \mathbf{w}_{\mathbf{k}'}^R(0) \quad (4.6)$$

and

$$\mathbf{u}_{\mathbf{k}}^R(0) = \int_{k'} [\coth \frac{\epsilon'}{2T} \text{Im} V_{\mathbf{k}-\mathbf{k}'}^R(-\epsilon') \frac{\partial \text{Re} G_{\mathbf{k}'}^R(\epsilon')}{\partial \epsilon'} + \tanh \frac{\epsilon'}{2T} \frac{\partial \text{Re} V_{\mathbf{k}-\mathbf{k}'}^R(-\epsilon')}{\partial \epsilon'} \text{Im} G_{\mathbf{k}'}^R(\epsilon')] (\mathbf{v}_{\mathbf{k}'} - \mathbf{v}_{\mathbf{k}}). \quad (4.7)$$

Here in the former equation we put $w_{\mathbf{k}'}^R(\epsilon')/(1 - \partial \Sigma_{\mathbf{k}'}^R(\epsilon')/\partial \epsilon')$ as $z_{\mathbf{k}'} w_{\mathbf{k}'}^R(0)$, because only the region of small ϵ' contributes to the integral owing to the factor $\partial G(\epsilon')/\partial \epsilon'$. The consistency between the numerical calculation and the analytical discussion in this section also verifies this replacement.

As often taken in the spin fluctuation theories,²⁴⁾ we use the following approximation to $V_{\mathbf{q}}^R(\omega)$,

$$V_{\mathbf{q}}^R(\omega) \simeq \frac{\chi(\mathbf{Q})}{1 + \xi^2(\mathbf{q} - \mathbf{Q})^2 - i\omega/\omega_{sf}}. \quad (4.8)$$

(ξ and ω_{sf} are the correlation length and the characteristic frequency of the antiferromagnetic spin fluctuation, respectively.) The following form of $G_{\mathbf{k}}^R(\epsilon)$ is also used,

$$G_{\mathbf{k}}^R(\epsilon) \simeq \frac{z_{\mathbf{k}}}{\epsilon - \xi_{\mathbf{k}}^* + i\gamma_{\mathbf{k}}}. \quad (4.9)$$

Then the integration in eq.(4.7) is carried out at $T \rightarrow 0$ and it can be shown that the term which includes $\text{Im} V^R$ vanishes and only the term which includes $\text{Im} G^R$ remains. The result is the following equation,

$$\mathbf{u}_{\mathbf{k}}^R(0) = \frac{\pi \chi(\mathbf{Q})}{2(2\pi)^2 v_F \xi} \int_{\text{FS}} dk' \frac{1}{\pi \xi} \frac{\mathbf{v}_{\mathbf{k}'} - \mathbf{v}_{\mathbf{k}}}{1/\xi^2 + (\mathbf{k} - \mathbf{k}' - \mathbf{Q})^2}. \quad (4.10)$$

Similarly we obtain

$$\mathbf{w}_{\mathbf{k}}^R(0) = \mathbf{u}_{\mathbf{k}}^R(0) + \frac{\pi z_{\mathbf{k}} \chi(\mathbf{Q})}{2(2\pi)^2 v_F \xi} \int_{\text{FS}} dk' \frac{1}{\pi \xi} \frac{\mathbf{w}_{\mathbf{k}'}^R(0)}{1/\xi^2 + (\mathbf{k} - \mathbf{k}' - \mathbf{Q})^2}. \quad (4.11)$$

(v_F is the velocity at the Fermi surface.) Then in the limit of $\xi \rightarrow \infty$ the integral in these equations reduces to the delta function $\delta(\mathbf{k} - \mathbf{k}' - \mathbf{Q})$. However, as ξ is not infinitely large in real systems, we introduce the reducing factor. Then the following equations are obtained.

$$\mathbf{w}_{\mathbf{k}}^R(0) = \mathbf{u}_{\mathbf{k}}^R(0) + z_{\mathbf{k}} c \alpha \mathbf{w}_{\mathbf{k}-\mathbf{Q}}^R(0), \quad (4.12)$$

and

$$\mathbf{u}_{\mathbf{k}}^R(0) = c(\alpha \mathbf{v}_{\mathbf{k}-\mathbf{Q}} - \mathbf{v}_{\mathbf{k}}). \quad (4.13)$$

Here $c := \frac{\pi\chi(\mathbf{Q})}{2(2\pi)^2 v_F \xi}$ and α is some constant which is the reducing factor owing to the momentum dependence of $V_{\mathbf{q}}^R(0)$ and $0 < \alpha < 1$. By using $(v_{\mathbf{k}-\mathbf{Q}_x}, v_{\mathbf{k}-\mathbf{Q}_y}) = -(v_{\mathbf{k}_y}, v_{\mathbf{k}_x})$, the above equations are solved as,

$$w_{\mathbf{k}_x}^R(0) = \frac{u_{\mathbf{k}_x}^R(0) - z c \alpha u_{\mathbf{k}_y}^R(0)}{1 - (z c \alpha)^2} \quad (4.14)$$

and

$$u_{\mathbf{k}_x}^R(0) = -c(v_{\mathbf{k}_x} + \alpha v_{\mathbf{k}_y}). \quad (4.15)$$

The equation for y -component is written by exchanging x with y in the above equations. To see the behavior of the current on the Fermi surface we analyze these equations on the typical three points, at two hot spots ($hs1$ and $hs2$) and at a cold spot (cs). The locations of these points are shown in Fig.3 of §5.

$$u_{\mathbf{k}_x}^R(0) \simeq -c v_{\mathbf{k}_x}, u_{\mathbf{k}_y}^R(0) \simeq -c \alpha v_{\mathbf{k}_x} \quad (\text{at } hs1), \quad (4.16)$$

$$u_{\mathbf{k}_x}^R(0) \simeq u_{\mathbf{k}_y}^R(0) \simeq -c(1 + \alpha)v_{\mathbf{k}_x} \quad (\text{at } cs), \quad (4.17)$$

$$u_{\mathbf{k}_x}^R \simeq -c \alpha v_{\mathbf{k}_y}, u_{\mathbf{k}_y}^R \simeq -c v_{\mathbf{k}_y} \quad (\text{at } hs2). \quad (4.18)$$

By using the above equations and $z \simeq (1 + c)^{-1}$, $c \gg 1$ we obtain

$$j_{\mathbf{k}_x}^* \simeq z_{\mathbf{k}} v_{\mathbf{k}_x} \quad (\text{at } hs1), \quad (4.19)$$

$$j_{\mathbf{k}_x}^* \simeq z_{\mathbf{k}} v_{\mathbf{k}_x} \quad (\text{at } cs), \quad (4.20)$$

$$j_{\mathbf{k}_x}^* \simeq \frac{-\alpha z_{\mathbf{k}} v_{\mathbf{k}_y}}{1 - \alpha^2} \quad (\text{at } hs2). \quad (4.21)$$

From the above equations we can see that the growth of the antiferromagnetic spin fluctuation described by α affects mainly near $hs2$. Then we can see that the reduction of $1/\lambda^2$ accompanied by the spin fluctuation is mainly caused by $hs2$. It can be said that this point is strongly affected by the Umklapp scattering as can be seen in fig.2.

On the other hand the temperature dependence of $1/\lambda^2$ at the low temperature is dominated by the point cs and $d\lambda^{-2}/dT|_{T=0}$ is determined by j^{*2} unlike j^* in the case of λ^{-2} at absolute zero. These properties are shown in the formula of $d\lambda^{-2}/dT$ at absolute zero derived from eqs.(2.2) and (2.4) as

$$\frac{d}{dT} \left(\frac{1}{\lambda_{\mu\nu}^2(T)} \right)_{T=0} \propto \int_{\text{FS}} \frac{dS_k}{2\pi^2 |\mathbf{v}^*(\mathbf{k})|} j_{\mu}^*(\mathbf{k}) \left(-\frac{dY(\mathbf{k}; T)}{dT} \right)_{T=0} j_{\nu}^*(\mathbf{k}). \quad (4.22)$$

In this equation the main contribution comes from near point cs because of the pairing symmetry of high- T_c cuprates. Then this equation indicates that the reduction of $1/\lambda^2(0)$ accompanied by the spin fluctuation does not mean that the reduction of $(d/dT)\lambda^{-2}(0)$ because j^* at cs is not affected by the growth of the spin fluctuation as can be seen from eq.(4.20). This is also confirmed numerically in §5.3.

4.3 Nature of Umklapp process

The large value of the Umklapp term in the case of strong antiferromagnetic spin fluctuation is understood by considering the extreme example as follows. If $V_{\mathbf{q}}(\omega)$ and $W_{\mathbf{q}}(\omega)$ are, respectively, replaced by $V\delta(\mathbf{q} - \mathbf{Q})\delta(\omega)$ and $W\delta(\mathbf{q} - \mathbf{Q})\delta(\omega)$, then $\mathbf{u}_{\mathbf{k}}(\epsilon)$ is written as

$$\begin{aligned}\mathbf{u}_{\mathbf{k}}(\epsilon) &= V \int_{k'} G_{\mathbf{k}-\mathbf{Q}}(\epsilon) G_{\mathbf{k}'-\mathbf{Q}}(\epsilon') \frac{\partial G_{\mathbf{k}'}(\epsilon')}{\partial \epsilon'} (\mathbf{v}_{\mathbf{k}} - \mathbf{v}_{\mathbf{k}-\mathbf{Q}}) \\ &= 2V \int_{k'} G_{\mathbf{k}-\mathbf{Q}}(\epsilon) G_{\mathbf{k}'-\mathbf{Q}}(\epsilon') \frac{\partial G_{\mathbf{k}'}(\epsilon')}{\partial \epsilon'} \mathbf{v}_{\mathbf{k}}.\end{aligned}\quad (4.23)$$

Here $\mathbf{v}_{\mathbf{k}-\mathbf{Q}}$ is replaced by $-\mathbf{v}_{\mathbf{k}}$.

As the \mathbf{q} -dependence of $V_{\mathbf{q}}(\omega)$ and $W_{\mathbf{q}}(\omega)$ is weakened, it is easily seen that the magnitude of the above $\mathbf{u}_{\mathbf{k}}(\epsilon)$ becomes small. On the other hand if $V_{\mathbf{q}}(\omega)$ and $W_{\mathbf{q}}(\omega)$ have sharp peaks at $\mathbf{q} = \mathbf{0}$, $\omega = 0$, i.e. in the case of strong ferromagnetic fluctuation, (though this is not the case of high- T_c , we consider it as just an example to illustrate the effect of the Umklapp scattering) it can be seen that the Umklapp term vanishes as below.

$$\begin{aligned}\mathbf{u}_{\mathbf{k}}(\epsilon) &= V \int_{k'} G_{\mathbf{k}}(\epsilon) G_{\mathbf{k}'}(\epsilon') \frac{\partial G_{\mathbf{k}'}(\epsilon')}{\partial \epsilon'} (\mathbf{v}_{\mathbf{k}} - \mathbf{v}_{\mathbf{k}}) \\ &= 0.\end{aligned}\quad (4.24)$$

These behaviors can be understood intuitively by drawing the processes like in Fig. 2. The

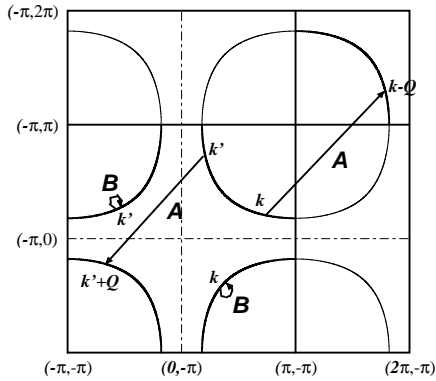


Fig. 2. The characteristic scattering processes with and without the Umklapp scattering

scattering process is $(k, k') \rightarrow (k - q, k' + q)$, and then by using the notation in this figure the case of the strong antiferromagnetic spin fluctuation corresponds to the case where the process of *A* dominates and the case of the strong ferromagnetic spin fluctuation corresponds to the case where the process of *B* is dominant. The process *A* is clearly the Umklapp process and the process *B*

means that the electron goes back to the beginning point on the Fermi surface and this process has no contribution to $\mathbf{u}_{\mathbf{k}}(\epsilon)$. Both processes are equally contained in the case where the momentum dependence of the irreducible four point vertex is weak. In the actual system both processes exists and which type of these processes is dominant is the factor for determining whether the current $j^* < v^*$ or not.

4.4 Backflow

In §2 it is shown that the backflow can be estimated from the two kinds of the derivative of self-energy by \mathbf{k} , $\partial\Sigma_{\mathbf{k}}^R(0)/\partial\mathbf{k}$ and $d\Sigma_{\mathbf{k}}^R(0)/d\mathbf{k}$. The integral equations which are obeyed by these quantity is written as follows;

$$\begin{aligned} \frac{\partial\Sigma_{\mathbf{k}}^R(0)}{\partial\mathbf{k}} &= \int_{k'} [\coth\frac{\epsilon'}{2T} \text{Im}V_{\mathbf{k}-\mathbf{k}'}^R(-\epsilon') \frac{\partial\text{Re}G_{\mathbf{k}'}^R(\epsilon')}{\partial\epsilon'} + \tanh\frac{\epsilon'}{2T} \frac{\partial\text{Re}V_{\mathbf{k}-\mathbf{k}'}^R(-\epsilon')}{\partial\epsilon'} \text{Im}G_{\mathbf{k}'}^R(\epsilon')] z_{\mathbf{k}'} \left(\mathbf{v}_{\mathbf{k}'} + \frac{\partial\Sigma_{\mathbf{k}'}^R(0)}{\partial k'} \right) \\ &+ \frac{\partial}{\partial\epsilon'} \left(\tanh\frac{\epsilon'}{2T} \right) \text{Re}V_{\mathbf{k}-\mathbf{k}'}^R(-\epsilon') \text{Im}G_{\mathbf{k}'}^R(\epsilon') \end{aligned} \quad (4.25)$$

and

$$\frac{d\Sigma_{\mathbf{k}}^R(0)}{d\mathbf{k}} = \int_{k'} [\coth\frac{\epsilon'}{2T} \text{Im}V_{\mathbf{k}-\mathbf{k}'}^R(-\epsilon') \frac{\partial\text{Re}G_{\mathbf{k}'}^R(\epsilon')}{\partial\epsilon'} + \tanh\frac{\epsilon'}{2T} \frac{\partial\text{Re}V_{\mathbf{k}-\mathbf{k}'}^R(-\epsilon')}{\partial\epsilon'} \text{Im}G_{\mathbf{k}'}^R(\epsilon')] z_{\mathbf{k}'} \left(\mathbf{v}_{\mathbf{k}'} + \frac{d\Sigma_{\mathbf{k}'}^R(0)}{dk'} \right). \quad (4.26)$$

Here $\Sigma_{\mathbf{k}'}^R(\epsilon')$ is replaced by $\Sigma_{\mathbf{k}'}^R(0)$ by considering that small ϵ' region dominates in the integral as before and terms including $W_{\mathbf{q}}(\omega)$ can be neglected for the same reason in the previous subsection. The main difference between the above two equation is the presence of the third term in eq.(4.25) and this is the difference between the k and ω -limits in the finite temperature formalism. The integral of the first term and the second term in eqs.(4.25) and (4.26) are carried out in the same way in eq.(4.7) and it can be seen that the third integration in eq.(4.25) has opposite sign and twice in magnitude as compared with the second one. Then the eqs.(4.25) and (4.26) reduce to

$$\frac{\partial\Sigma_{\mathbf{k}}^R(0)}{\partial\mathbf{k}} = -cz_{\mathbf{k}}\alpha(\mathbf{v}_{\mathbf{k}-\mathbf{Q}} + \frac{\partial\Sigma_{\mathbf{k}-\mathbf{Q}}^R(0)}{\partial\mathbf{k}}) \quad (4.27)$$

and

$$\frac{d\Sigma_{\mathbf{k}}^R(0)}{d\mathbf{k}} = cz_{\mathbf{k}}\alpha(\mathbf{v}_{\mathbf{k}-\mathbf{Q}} + \frac{\partial\Sigma_{\mathbf{k}-\mathbf{Q}}^R(0)}{\partial\mathbf{k}}). \quad (4.28)$$

By applying the argument in §4.2 to the above equations we obtain the following behavior of these.

$$\frac{\partial\Sigma_{\mathbf{k}}^R(0)}{\partial k_x} \simeq \frac{\alpha(v_{\mathbf{k}_y} + \alpha v_{\mathbf{k}_x})}{1 - \alpha^2}, \quad (4.29)$$

$$\frac{d\Sigma_{\mathbf{k}}^R(0)}{dk_x} \simeq \frac{\alpha(-v_{\mathbf{k}_y} + \alpha v_{\mathbf{k}_x})}{1 - \alpha^2}. \quad (4.30)$$

Then the backflow defined in §2 is derived as follows.

$$\frac{B\mathbf{k}_x}{z_{\mathbf{k}}} \simeq -\frac{2\alpha v_{\mathbf{k}_y}}{1 - \alpha^2}. \quad (4.31)$$

From these equations it can be seen that the backflow is negative in the case of $v_{\mathbf{k}_y} \geq 0$ and the magnitude of this becomes large as the spin fluctuation grows (i.e. α has the larger value). These considerations indicate that $j_{\mathbf{k}_x}^*$ is smaller than $v_{\mathbf{k}_x}^*$ in magnitude and $\lambda^{-2} \leq 4\pi e^2 n/m^*$ follows this.

§5. Results of Numerical Calculation

In this section we present the results of numerical calculations based on the model and approximation presented in the previous section.

The first Brillouin zone is divided into 128×128 mesh and the roughness in the following figures of the Fermi surface and the velocity is caused by this mesh structure. The hole doping level is taken as $\delta = 0.15$ in the figure with no indication.

Firstly (a quarter of) the Fermi surfaces in the first Brillouin zone with the hole doping $\delta = 0.15$, calculated with SC-SOPT and FLEX approximations are shown in Fig. 3. In this figure *hs1*

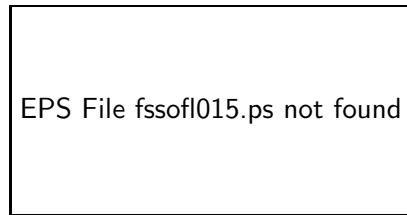


Fig. 3. Fermi surfaces with the hole doping $\delta = 0.15$, calculated by using SC-SOPT and FLEX approximations.

and *hs2* mean the hot spots which are the intersection points between the Fermi surface and the magnetic Brillouin zone (the line connecting $(\pi, 0)$ with $(0, \pi)$ in this figure). These are the points connected by other points on Fermi surface by the vector $\mathbf{Q} = (\pi, \pi)$, and *cs* means the cold spot which is the point (on the Fermi surface) most far from the magnetic Brillouin zone. These notations are the same as in some papers on high- T_c cuprates.⁹⁾ It is also known that the Fermi surface is deformed by the correlation effect. From this figure it is noted that one with FLEX is deformed much to the magnetic Brillouin zone than the other with SC-SOPT. This is because the FLEX approximation includes the effect of the spin fluctuation effect much.

5.1 Momentum dependence of the current

From here the only x -component of the vector is shown in the figure. The y -component at (k_x, k_y) is identified with the x -component at (k_y, k_x) . $j_{\mathbf{k}_x}^*$ in SC-SOPT is shown in Fig.4(a) with

renormalized velocity $v_{\mathbf{k}_x}^*$ and bare velocity $v_{\mathbf{k}_x}$. From the argument given in §4.1 the current



Fig. 4. The momentum dependence of $j_{\mathbf{k}_x}^*$, $v_{\mathbf{k}_x}^*$ and $v_{\mathbf{k}_x}$ in (a) SC-SOPT and (b) FLEX

$j_{\mathbf{k}_x}^*$ is not expected to be much different from $v_{\mathbf{k}_x}^* \simeq z_{\mathbf{k}} v_{\mathbf{k}_x}$ and this expectation is verified. The term $\partial\Sigma_{\mathbf{k}}(0)/\partial k_x$ in the renormalized velocity $v_{\mathbf{k}_x}^*$ is negligible in the case of weak momentum dependence of the irreducible four point vertex. To put it more precisely, replacing $j_{\mathbf{k}_x}^*$ by $v_{\mathbf{k}_x}^*$, like in ref.3, is not verified exactly but only approximately with a condition given above on the irreducible four point vertex. $j_{\mathbf{k}_x}^*$ in FLEX is shown in Fig.4(b). From this figure it can be seen that the current is different so much from the renormalized velocity, unlike in the case of SC-SOPT, owing to the strong spin fluctuation. There are two reasons of this difference. One is that $j_{\mathbf{k}_x}^*$ is reduced by the large negative value of $w_{\mathbf{k}_x}$ which originates from the large $u_{\mathbf{k}_x}$. The other is that $v_{\mathbf{k}_x}^*$ increases due to the positive value of $\partial\Sigma_{\mathbf{k}}(0)/\partial k_x$. The latter point manifests itself in $v_{\mathbf{k}_x}^* > v_{\mathbf{k}_x}$ at $hs2$. Both of these originate from the large spin fluctuation and in this case it is not allowed to approximate $j_{\mathbf{k}_x}^* \simeq z_{\mathbf{k}} v_{\mathbf{k}_x}$, as in SC-SOPT. The above mentioned difference between $j_{\mathbf{k}_x}^*$ and $v_{\mathbf{k}_x}^*$ also numerically verifies the discussion on the backflow in §4.4.

5.2 λ^{-2}

Based on the above behaviors of $j_{\mathbf{k}_x}^*$ the doping dependence of λ^{-2} is presented. The result of SC-SOPT is shown in Fig.5(a). From this figure it can be seen that λ^{-2} , which is proportional

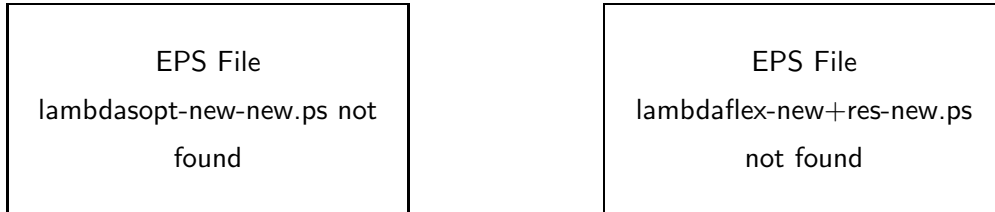


Fig. 5. The integrals over the Fermi surface, $\int_{\text{FS}} \frac{dk}{2\pi^2 |v_{\mathbf{k}}^*|} v_{\mathbf{k}_x}^* X$, in (a) SC-SOPT and (b) FLEX. Here $X = j_{\mathbf{k}_x}^*$, $z_{\mathbf{k}} v_{\mathbf{k}_x}$ and $v_{\mathbf{k}_x}$.

to the case of $X = j_{\mathbf{k}_x}^*$, is approximately described by n/m^* , which is proportional to the case

of $X = z_{\mathbf{k}} v_{\mathbf{k}_x}$. This is because the momentum dependence of the irreducible four point vertex is weak as discussed in §3 and §4.1. It is also noted that the value of the case $X = v_{\mathbf{k}_x}$ decreases as the hole doping δ increases. This is because the case $X = v_{\mathbf{k}_x}$ corresponds to n/m , n means the effective carrier and increases owing to the increase of the effective carrier density $1 - \delta$. ($\delta = 0$ means the half-filled case and therefore the effective carrier density is 1.) The decrease of n/m as δ increases indicates that $n/m^* = zn/m$ (the case of $X = v_{\mathbf{k}_x}^*$) also decreases because the doping dependence of z is rather weaker than the change of n . The above results are considered to explain the experimental doping dependence of λ^{-2} in the overdoped region because the perturbation scheme is valid due to the weakness of the spin fluctuation in this region. The calculations by FLEX is shown in Fig.5(b). Unlike the case of SC-SOPT, it can be seen that the value and the doping dependence of the case $X = j_{\mathbf{k}_x}^*$ is very different from those of the case $X = z_{\mathbf{k}} v_{\mathbf{k}_x}$. This is because the spin fluctuation highly renormalizes the current. The doping dependence of the case $X = z_{\mathbf{k}} v_{\mathbf{k}_x}$ is rather weak compared with the case of SC-SOPT owing to decreasing of the renormalization factor in the low doping. On the other hand the value of the case $X = j_{\mathbf{k}_x}^*$ decreases as the δ decreases because the spin fluctuation grows in the low doping region. This behavior of λ^{-2} (the case of $X = j_{\mathbf{k}_x}^*$) is considered to explain the experimental doping dependence in the optimal and the underdoped regions.

While the physical meaning and a justification of the usage of the perturbation theory on the overdoped region and the spin fluctuation theory on the optimal and the underdoped regions is discussed in §7, we discuss the following two points. One of these is that by discussing the above results conversely, it can be said that the peak at the slightly overdoped region not at the optimal doping as experimentally observed suggest that the spin fluctuation begins to grow in this region, and therefore this is reflected in other quantities like the one-particle spectrum.¹¹⁾ The other is about the renormalization factor z . The calculated z by SC-SOPT and FLEX are not smoothly connected. This suggests that the higher order terms in the perturbation expansion are needed to calculate the doping level itself of the peak in λ^{-2} as discussed in §7, while the explanation on the behaviors of λ^{-2} on both sides of the peak is not modified.

5.3 On the slope of λ^{-2} at absolute zero

In high- T_c cuprates it is known that at the low temperature λ^{-2} decreases linearly with T because of the line nodes in the superconducting gap. If we assume the isotropic case, the value of λ^{-2} at $T = 0$ is given by,

$$\lambda^{-2} \propto \frac{n}{m^*} \left(1 + \frac{F_1^s}{2} \right), \quad (5.1)$$

which comes from the fact that λ^{-2} is linear in j^* . On the other hand from eq.(4.22) it can be seen that the coefficient of T in λ^{-2} at the low temperature is given by

$$\frac{d\lambda^{-2}}{dT} \propto \frac{n}{m^*} \left(1 + \frac{F_1^s}{2} \right)^2, \quad (5.2)$$

which comes from the fact that $d\lambda^{-2}/dT$ is square in j^* in this case. Then it is expected that if the decreasing of λ^{-2} is attributed to small $1 + F_1^2/2$ as δ decreases, then the rate of decreasing of $d\lambda^{-2}/dT$ is expected to be more rapid than λ^{-2} owing to $(1 + F_1^2/2)^2$. This expectation is denied by the experimental results (*e.g.* refs.25 and 26). Here we clarify that this failure in the explanation for the experiments is not caused by the failure of the explanation based on the Fermi liquid theory but owing to the use of the isotropic model which is unrealistic as understood from the previous sections.

The slope $d\lambda^{-2}/dT$ at $T = 0$ comes from the derivative of Yosida function by the temperature $dY(\mathbf{k};T)/dT$. From the fact that the excitations of the quasiparticles at the low temperature are mainly produced at the line nodes (which are equal to the cold spots in our system), $dY(\mathbf{k};T)/dT$ has a large value at these points. Therefore it is allowed to consider the function $j_{\mathbf{k}}^{*2}$ only at the cold spots in $d\lambda^{-2}/dT|_{T=0}$. On the other hand for the value of λ^{-2} at $T = 0$ the whole value of $v_{\mathbf{k}_x}^* j_{\mathbf{k}_x}^*$ on the Fermi surface should be considered in practice.

With the above consideration in mind we present the momentum dependence of $j_{\mathbf{k}_x}^*$ at hole doping $\delta = 0.10$ and $\delta = 0.20$ in Fig.6(a). From this figure it can be seen that the doping

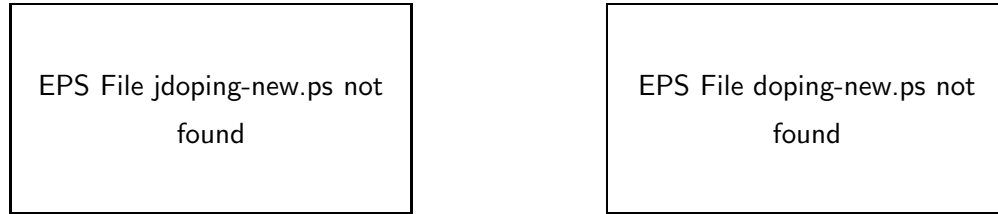


Fig. 6. (a) The momentum dependence of $j_{\mathbf{k}_x}^*$ at $\delta = 0.10$ and $\delta = 0.20$ in FLEX. (b) The doping dependence of $j_{\mathbf{k}_x}^*$ at the characteristic points $hs1$, cs and $hs2$ on Fermi surface in FLEX.

dependence of the current $j_{\mathbf{k}_x}^*$ around $\mathbf{k} = hs2$ is large while those around $\mathbf{k} = hs1, cs$ is weak. The doping dependences at these points are shown in Fig.6(b). From these figures it can be seen that the decrease of λ^{-2} at $T = 0$ presented in fig.5(b) is caused by the decrease of $j_{\mathbf{k}_x}^*$ around the points $hs2$ while $j_{\mathbf{k}_x}^*$ around the points $hs1$ and cs doesn't contribute so much on the doping dependence of this quantity. On the other hand the small doping dependence of $j_{\mathbf{k}_x}^*$ around cs is reflected in the small doping dependence of $d\lambda^{-2}/dT$. These behaviors of $j_{\mathbf{k}_x}^*$, with the anisotropy included, are considered to explain the experimental results of λ^{-2} and $d\lambda^{-2}/dT$ consistently.

§6. Relation between Magnetic Field Penetration Depth and Superconducting Fluctuation

The high- T_c cuprates is known to show the pseudogap phenomena in the underdoped region. Some authors are tried to explain this phenomenon by relating this with large value of the magnetic

field penetration depth.⁴⁾ The point of their argument is that by writing the phase only model the phase stiffness is proportional to the inverse of squared magnetic field penetration depth and then the large value of λ at *absolute zero* in the underdoped region means that the phase fluctuation is dominant in this region. In this section we investigate whether this assertion is correct.

The GL model is written as

$$\mathcal{H} = \int d\mathbf{r} \left[a(\epsilon_0|\psi|^2 + \xi_0^2|(-i\nabla + \frac{2\pi}{\Phi_0}\mathbf{A})\psi|^2) + \frac{b}{2}|\psi|^4 \right]. \quad (6.1)$$

Here $a := \rho^*(0)$ ($\rho^*(0)$ is the density of states at Fermi level enhanced by $1/z$), $\epsilon_0 := (T - T_c)/T_c$, $\xi_0 := \frac{7\zeta(3)}{48} \left(\frac{v_F}{\pi T_c} \right)^2$, Φ_0 is the flux quantum and $b := \frac{7\zeta(3)}{8} \frac{\rho^*(0)}{(\pi T_c)^2}$ by the microscopic calculation with an usual model where the attractive force is operated between renormalized quasiparticles. By using $\psi = |\psi|e^{i\phi}$ this model is reduced to a phase only model,

$$\mathcal{H} = \int d\mathbf{r} \left[-\frac{a|\epsilon_0|^2}{2b} + \frac{1}{8\pi}\lambda^{-2}(T) \left(\mathbf{A} + \frac{\Phi_0}{2\pi}\nabla\phi \right)^2 \right]. \quad (6.2)$$

Here we put

$$\lambda^{-2}(T) = \left(\frac{2\pi\xi_0}{\Phi_0} \right)^2 \frac{8\pi a^2 |\epsilon_0|}{b}. \quad (6.3)$$

From this expression with the above parameter inserted it is seen that the λ^{-2} is proportional to z . This is in contrast to $\lambda^{-2} \propto z(1 + F_1^s/2)$ at absolute zero discussed in the previous sections. On the other hand, from eqs.(2.2) and (2.5) the magnetic field penetration depth near the transition temperature is given by

$$\frac{1}{\lambda_{\mu\nu}^2(T \simeq T_c)} \propto \int_{\text{FS}} \frac{dS_k}{2\pi^2 |\mathbf{v}^*(\mathbf{k})|} v_\mu^*(\mathbf{k})(1 - Y(\mathbf{k}; T))v_\nu^*(\mathbf{k}). \quad (6.4)$$

ϵ_0 term is derived from $1 - Y(\mathbf{k}; T)$ and we neglected the second term in the right hand side of eq.(2.5) due to the smallness of $1 - Y(\mathbf{k}; T)$ near T_c . From this equation $\lambda^{-2}(T \simeq T_c)$ is proportional to the renormalization factor z and this is consistent with the eq.(6.3) not with the expression of λ^{-2} at $T = 0$. This suggests that F_1^s term which is one of the particle-hole four point vertices is not effective near T_c where the particle-particle four point vertex is remarkable, although this notion is much simplified and should be elaborate for the exact description.

The above consideration indicates that the the smallness of the coefficient in the phase only model cannot be identified with the smallness of λ^{-2} at the absolute zero even if the temperature dependence ϵ_0 is excluded. This is originated from the fact that there is a non trivial temperature dependence in the vertex correction in the superconducting state. Therefore the small λ^{-2} at absolute zero doesn't necessarily indicate that the thermal fluctuation around T_c is large because the renormalization factor in the phase model is not $z(1 + F_1^s/2)$ but z . Then the the small λ^{-2} cannot be directly related with large thermal fluctuation in the underdoped region although it is considered that the thermal fluctuation is large as experiments indicate, but the origin of the large fluctuation is composed of the factors like the strong coupling effect and the quasi two dimensionality.⁷⁾

§7. Summary and Discussion

In this paper we derived the general expression for the effect of the Umklapp scattering on the current and discussed the magnetic field penetration depth, particularly of high- T_c cuprates, both analytically and numerically.

In §2 a formula for the current carried by quasiparticles which explicitly expresses the effect of the Umklapp scattering is derived. This is basically derived from the usual expression for the current written by the renormalized velocity with the backflow. However to see the effect of the Umklapp scattering the above two quantities are not basic but this effect is written by the integrals over the whole energy scale not only over the Fermi surfaces. This is the basic difference between the current in the hydrodynamic region and in the collisionless region, and indicates that the backflow term is not necessarily the basic quantity in the lattice system. The advantages of our expression for the Umklapp term over the notion of the backflow are the followings. We can show that the upper limit for the current is the bare velocity and doesn't exceed this value and that the correlation effect is unified in the Umklapp term while by using the backflow notion the renormalized velocity also includes the correlation effect.

In §4 the Umklapp term, mainly of the high- T_c cuprates, is analytically discussed. In the highly overdoped region of the high- T_c cuprates the momentum dependence of the irreducible four point vertex is weak though it exists, and by neglecting this small term the Umklapp term is written only by the self-energy term. Therefore the current is expressed only by the product of the renormalization factor and the bare velocity and then the λ^{-2} is proportional to n/m^* . By this fact the reason why a misunderstanding of $\lambda^{-2} \propto n/m^*$ like ref.3 has not been confronted with a difficulty so far is understood. In the optimal and underdoped regions it is known that there exists the strong spin fluctuation, and the temperature-linear resistivity and the temperature dependent Hall coefficient can be derived by using this feature. Therefore it is reasonable to start with the spin fluctuation model to discuss the magnetic field penetration depth too. It is found that the strong momentum dependence of the irreducible four point vertex induces the large vertex correction in addition to the self-energy term and this correction makes the Umklapp term dependent on the points on the Fermi surface. Therefore at some points the current is not written by the product of the renormalization factor and the bare velocity unlike the case of the highly overdoped region, but reflects the strong Umklapp scattering at these points. These considerations indicate that the strong antiferromagnetic spin fluctuation can be identified with the strong Umklapp scattering as the effect on the current. The other characteristic results are that the backflow always takes an opposite sign to the bare velocity and the partial derivative of the self-energy by the momentum takes the same sign as the bare velocity with non-negligible magnitude. The latter point indicates that the renormalized velocity is not so simple and supports the above assertion that the dividing the current to the renormalized velocity and the backflow is not useful.

The main results obtained by numerical calculations in §5 are that the doping dependence of λ^{-2} in experiments can be explained by using the perturbation scheme in the overdoped region and the spin fluctuation theory in the optimal and underdoped regions, and that the relation between λ^{-2} and $d\lambda^{-2}/dT$ at absolute zero indicated by experiments, which was failed to explain by the isotropic model,¹³⁾ is explained by using the anisotropic model based on the spin fluctuation theory. As regards with the latter point the way to recover the consistency between these two quantities based on the isotropic model is indicated in ref.25 by using the angle resolved photo-emission spectroscopy (ARPES) experiments. It is summarized as that ARPES experiments indicate that the form of the gap function deforms from the $d_{x^2-y^2}$ -pairing with underdoping and this suggests that the magnitude of the gap around the cold spot decreases and then the excitations around this point increases with underdoping. Although this behavior may be possible in the underdoped region, the calculated gap with the FLEX approximation suggests that the deformation from the $d_{x^2-y^2}$ -pairing is not so drastic as this experiments suggests. While one of the reasons for this is the inaccuracy of the approximation, the other is that the ARPES experiments at the cold spot where the dispersion is sharp, cannot be accurate to discuss the form of the gap function around the node because of the limited resolution in ARPES. In spite of these facts the anisotropy of the system is not obviously negligible and it is needed for considering the qualitative estimation for $d\lambda^{-2}/dT$.

The explanation on the doping dependence of λ^{-2} needs some notions. It is desirable not to rely on the specific approximations, but this cannot be done. Then it is needed to consider what is physically the most appropriate method. Because we stand upon the Fermi liquid theory, the perturbation scheme should be taken at first. In high- T_c cuprates the on-site Coulomb interaction in the Hubbard model is large, and then it may be considered that all higher order terms is effective in the expansion. The reason why the some low order terms is sufficient in the overdoped region and the spin fluctuation theory is appropriate (only approximately) in the optimal and the underdoped region, is explained as follows. In the study on the single impurity system, it is shown that in the perturbation expansion by the on-site Coulomb interaction U , the coefficient of U^n (n is the order of the expansion) becomes smaller as n becomes large.²⁷⁾ This indicate that it is practically sufficient to take only the low order terms in U , even if U is somewhat large, in contrast to the mean field treatment. The notable point is that there is no momentum dependence in the single impurity system. This indicate that it is reasonable to take the low order perturbation scheme as an approximation in the overdoped region where the momentum dependence of the vertex is rather weak owing to its filling. With underdoping the momentum dependence of the vertex becomes strong because the system approaches to the antiferromagnetic phase. Therefore in this case taking only the low order terms is not appropriate owing to the fact that the cancellation between higher order terms is not effective, but the specific mode is considered to be effective up to higher order

terms and this leads to the antiferromagnetic spin fluctuation. This is the reason why we take the spin fluctuation theory as an approximation in the optimal and underdoped regions. It is also the reason why FLEX approximation is inappropriate in the overdoped region because other higher order terms which should cancel the RPA type terms in the case of the weak momentum dependence are not included. The above qualitative discussions should be verified by explicitly calculating the higher order terms with various doping levels. This is an important feature problem.

The other notions with the FLEX approximation is that this approximation is not good to describe the Mott transition.²⁸⁾ The main fault of this approximation is lack of the Hubbard peaks in the density of states.²⁹⁾ However it is the momentum dependence at the low energy that is important for our explanation on the current and the magnetic field penetration depth, and therefore main results in this paper is not changed qualitatively by the existence of the high-energy structure like the Hubbard peak while the improvement of the density of states would slightly affect the quantitative results.

Acknowledgment

Numerical computation in this work was carried out at the Yukawa Institute Computer Facility.

Appendix: Expressions at Finite Temperature

At finite temperature the corresponding equation of eq.(2.20) is ($\mathbf{w}_{\mathbf{k}}^R(\epsilon) := \frac{d\Sigma_{\mathbf{k}}^R(\epsilon)}{d\mathbf{k}} + \frac{\partial\Sigma_{\mathbf{k}}^R(\epsilon)}{\partial\epsilon}\mathbf{v}_{\mathbf{k}}$),

$$\begin{aligned} \mathbf{w}_{\mathbf{k}}^R(\epsilon) &= \frac{1}{2i} \int_{k'} \left[\Im_{\mathbf{k},\mathbf{k}'}^{(11)}(\epsilon, \epsilon') \left(-\frac{\partial G_{\mathbf{k}'}^R(\epsilon')}{\partial\epsilon'} \right) + \Im_{\mathbf{k},\mathbf{k}'}^{(13)}(\epsilon, \epsilon') \left(-\frac{\partial G_{\mathbf{k}'}^A(\epsilon')}{\partial\epsilon'} \right) \right] (\mathbf{v}_{\mathbf{k}'} - \mathbf{v}_{\mathbf{k}}) \\ &\quad - \int_{k'} \frac{1}{2T} \frac{1}{\cosh^2\epsilon'/2T} \Gamma_{\mathbf{k},\mathbf{k}'}^{(12)}(\epsilon, \epsilon') \text{Im}G_{\mathbf{k}'}^R(\epsilon') (\mathbf{v}_{\mathbf{k}'} - \mathbf{v}_{\mathbf{k}}) \\ &\quad + \frac{1}{2i} \int_{k'} \left[\Im_{\mathbf{k},\mathbf{k}'}^{(11)}(\epsilon, \epsilon') \left(-\frac{\partial G_{\mathbf{k}'}^R(\epsilon')}{\partial\epsilon'} \right) \frac{\mathbf{w}_{\mathbf{k}'}^R(\epsilon')}{1 - \partial\Sigma_{\mathbf{k}'}^R(\epsilon')/\partial\epsilon'} + \Im_{\mathbf{k},\mathbf{k}'}^{(13)}(\epsilon, \epsilon') \left(-\frac{\partial G_{\mathbf{k}'}^A(\epsilon')}{\partial\epsilon'} \right) \frac{\mathbf{w}_{\mathbf{k}'}^A(\epsilon')}{1 - \partial\Sigma_{\mathbf{k}'}^A(\epsilon')/\partial\epsilon'} \right] \\ &\quad - \int_{k'} \frac{1}{2T} \frac{1}{\cosh^2\epsilon'/2T} \Gamma_{\mathbf{k},\mathbf{k}'}^{(12)}(\epsilon, \epsilon') \text{Im}G_{\mathbf{k}'}^R(\epsilon') \frac{\mathbf{w}_{\mathbf{k}'}^R(\epsilon')}{1 - \partial\Sigma_{\mathbf{k}'}^R(\epsilon')/\partial\epsilon'}. \end{aligned} \quad (\text{A}\cdot 1)$$

Here the meanings of (11), etc. of \Im are same as in Éliashberg's paper³⁰⁾ and these are

$$\Im_{\mathbf{k},\mathbf{k}'}^{(11)}(\epsilon, \epsilon') = \tanh\frac{\epsilon'}{2T} [\Gamma_{\mathbf{k},\mathbf{k}'}^{(a)}(\epsilon, \epsilon') + \Gamma_{\mathbf{k},\mathbf{k}'}^{(b)}(\epsilon, \epsilon')] + 2i \cosh\frac{\epsilon - \epsilon'}{2T} \Delta_{\mathbf{k},\mathbf{k}'}^{(a)}(\epsilon, \epsilon'), \quad (\text{A}\cdot 2)$$

$$\frac{\partial\Im_{\mathbf{k},\mathbf{k}'}^{(12)}(\epsilon, \epsilon'; \omega)}{\partial\omega} \Big|_{\omega=0} = \frac{1}{2T} \frac{1}{\cosh^2\epsilon'/2T} \Gamma_{\mathbf{k},\mathbf{k}'}^{(12)}(\epsilon, \epsilon') \quad (\text{A}\cdot 3)$$

$$= \frac{1}{2T} \frac{1}{\cosh^2\epsilon'/2T} [\Gamma_{\mathbf{k},\mathbf{k}'}^{(a)}(\epsilon, \epsilon') + \Gamma_{\mathbf{k},\mathbf{k}'}^{(b)}(\epsilon, \epsilon')] \quad (\text{A}\cdot 4)$$

and

$$\Im_{\mathbf{k},\mathbf{k}'}^{(13)}(\epsilon, \epsilon') = -\tanh\frac{\epsilon'}{2T} [\Gamma_{\mathbf{k},\mathbf{k}'}^{(a)}(\epsilon, \epsilon') + \Gamma_{\mathbf{k},\mathbf{k}'}^{(b)}(\epsilon, \epsilon')] + 2i \cosh\frac{\epsilon + \epsilon'}{2T} \Delta_{\mathbf{k},\mathbf{k}'}^{(b)}(\epsilon, \epsilon'). \quad (\text{A}\cdot 5)$$

Then

$$\begin{aligned}
w_{\mathbf{k}}^R(\epsilon) &= \mathbf{u}_{\mathbf{k}}^R(\epsilon) + \int_{k'} \left\{ \tanh \frac{\epsilon'}{2T} \frac{\partial}{\partial \epsilon'} [\Gamma_{\mathbf{k}, \mathbf{k}'}^{(a)}(\epsilon, \epsilon') + \Gamma_{\mathbf{k}, \mathbf{k}'}^{(b)}(\epsilon, \epsilon')] \text{Im} G_{\mathbf{k}'}^R(\epsilon) \frac{w_{\mathbf{k}'}^R(\epsilon')}{1 - \partial \Sigma_{\mathbf{k}'}^R(\epsilon') / \partial \epsilon'} \right. \\
&\quad \left. - \coth \frac{\epsilon - \epsilon'}{2T} \Delta_{\mathbf{k}, \mathbf{k}'}^{(a)}(\epsilon, \epsilon') \frac{\partial G_{\mathbf{k}'}^R(\epsilon')}{\partial \epsilon'} \frac{w_{\mathbf{k}'}^R(\epsilon')}{1 - \partial \Sigma_{\mathbf{k}'}^R(\epsilon') / \partial \epsilon'} - \coth \frac{\epsilon + \epsilon'}{2T} \Delta_{\mathbf{k}, \mathbf{k}'}^{(b)}(\epsilon, \epsilon') \frac{\partial G_{\mathbf{k}'}^A(\epsilon')}{\partial \epsilon'} \frac{w_{\mathbf{k}'}^A(\epsilon')}{1 - \partial \Sigma_{\mathbf{k}'}^R(\epsilon') / \partial \epsilon'} \right\}.
\end{aligned} \tag{A.6}$$

Here we put $\Gamma_{\mathbf{k}, \mathbf{k}'}^{(a,b)}(\epsilon, \epsilon') = \text{Re} \Gamma_{\mathbf{k}, \mathbf{k}'}^{(a,b)}(\epsilon, \epsilon') + i \Delta_{\mathbf{k}, \mathbf{k}'}^{(a,b)}(\epsilon, \epsilon')$ as the four-point vertex which has a discontinuity along the cut $\text{Im}(\epsilon - \epsilon') = 0$ or $\text{Im}(\epsilon + \epsilon') = 0$ for the case of (a) or (b) in superscript, respectively. $\mathbf{u}_{\mathbf{k}}^R(\epsilon)$ has the following form and it is seen that this quantity vanishes in the absence of Umklapp process.

$$\begin{aligned}
\mathbf{u}_{\mathbf{k}}^R(\epsilon) &= \int_{k'} \left\{ \coth \frac{\epsilon - \epsilon'}{2T} \Delta_{\mathbf{k}, \mathbf{k}'}^{(a)}(\epsilon, \epsilon') \frac{\partial G_{\mathbf{k}'}^R(\epsilon')}{\partial \epsilon'} + \coth \frac{\epsilon + \epsilon'}{2T} \Delta_{\mathbf{k}, \mathbf{k}'}^{(b)}(\epsilon, \epsilon') \frac{\partial G_{\mathbf{k}'}^A(\epsilon')}{\partial \epsilon'} \right. \\
&\quad \left. - \tanh \frac{\epsilon'}{2T} \frac{\partial}{\partial \epsilon'} [\Gamma_{\mathbf{k}, \mathbf{k}'}^{(a)}(\epsilon, \epsilon') + \Gamma_{\mathbf{k}, \mathbf{k}'}^{(b)}(\epsilon, \epsilon')] \text{Im} G_{\mathbf{k}'}^R(\epsilon') \right\} (\mathbf{v}_{\mathbf{k}} - \mathbf{v}_{\mathbf{k}'}).
\end{aligned} \tag{A.7}$$

$$\begin{aligned}
&= - \int_{k'} \int_q \int \frac{dx}{\pi} \frac{\cosh \frac{x - \omega + \epsilon}{2T}}{\cosh \frac{\omega - \epsilon}{2T} \cosh \frac{\epsilon'}{2T} \cosh \frac{\epsilon' + x}{2T}} |\Gamma_{\mathbf{k}, \mathbf{k}', \mathbf{q}}(\epsilon, \epsilon', \omega, x)|^2 \\
&\quad \times \frac{\text{Im} G_{\mathbf{k}-\mathbf{q}}^R(\epsilon - \omega) \text{Im} G_{\mathbf{k}'}^R(\epsilon') \text{Im} G_{\mathbf{k}'+\mathbf{q}}^R(\epsilon' + x)}{(x - \omega - i\delta)^2} (\mathbf{v}_{\mathbf{k}-\mathbf{q}} + \mathbf{v}_{\mathbf{k}'+\mathbf{q}} - \mathbf{v}_{\mathbf{k}'} - \mathbf{v}_{\mathbf{k}}).
\end{aligned} \tag{A.8}$$

From eq.(A.7) to eq.(A.8) we used the spectral representation

$$G_{\mathbf{k}}^R(\epsilon) = \int \frac{dx}{\pi} \frac{\text{Im} G_{\mathbf{k}}^R(x)}{x - \epsilon - i\delta} \tag{A.9}$$

(here δ is positive infinitesimal quantity) and the trivial relation between hyperbolic functions

$$\left(\cosh \frac{x}{2T} - \tanh \frac{\omega - \epsilon}{2T} \right) \left(\tanh \frac{\epsilon'}{2T} - \tanh \frac{x + \epsilon'}{2T} \right) = - \frac{\cosh \frac{x - \omega + \epsilon}{2T}}{\cosh \frac{\omega - \epsilon}{2T} \cosh \frac{\epsilon'}{2T} \cosh \frac{\epsilon' + x}{2T}} \tag{A.10}$$

From eq.(A.6) and eq.(A.8) it is obvious that in the continuum $w_{\mathbf{k}}^R(\epsilon) = 0$ also holds at finite temperature as derived at absolute zero in §2. By taking the SC-SOPT and FLEX approximations as example the validity of the above equation can be confirmed. In the latter approximation it is needed to use the exact relation $\text{Im} V_{\mathbf{q}}^R(\omega) = W_{\mathbf{q}}(\omega) \text{Im} \chi_{\mathbf{q}}^R(\omega)$.

-
- [1] H. Takagi, T. Ito, S. Ishibashi, M. Uota, S. Uchida and Y. Tokura: Phys. Rev. B **40** (1989) 2254.
 - [2] J. Takeda, T. Nishikawa and M. Sato: Physica C **231** (1994) 293.
 - [3] Y. J. Uemura, G. M. Luke, B. J. Sternlieb, J. H. Brewer, J. F. Carolan, W. N. Hardy, R. Kadono, J. R. Kempton, R. F. Kiefl, S. R. Kreitzman, P. Mulhern, T. M. Riseman, D. L. Williams, B. X. Yang, S. Uchida, H. Takagi, J. Gopalakrishnan, A. W. Sleight, M. A. Subramanian, C. L. Chien, M. Z. Cieplak, Gang Xiao, V. Y. Lee, B. W. Statt, C. E. Stronach, W. J. Kossler and X. H. Yu: Phys. Rev. Lett. **62** (1989) 2317.
 - [4] V. J. Emery and S. A. Kivelson: Nature **374** (1995) 434.
 - [5] T. Moriya, Y. Takahashi and K. Ueda: J. Phys. Soc. Jpn. **59** (1990) 2905.

- [6] H. Kohno and K. Yamada: Prog. Theor. Phys. **85** (1991) 13.
- [7] T. Jujo and K. Yamada: J. Phys. Soc. Jpn. **68** (1999) 2198., T. Jujo, Y. Yanase and K. Yamada: *ibid.* **69** (2000) 2240.
- [8] S. Koikegami and K. Yamada: J. Phys. Soc. Jpn. **69** 768., Y. Yanase and K. Yamada: J. Phys. Soc. Jpn. **70** (2001) 1659.
- [9] H. Kontani, K. Kanki and K. Ueda: Phys. Rev. B **59** (1999) 14723; K. Kanki and H. Kontani: J. Phys. Soc. Jpn. **68** (1999) 1614.
- [10] P. A. Lee and X.-G. Wen: Phys. Rev. Lett. **78** (1997) 4111.
- [11] D. L. Feng, D. H. Lu, K. M. Shen, C. Kim, H. Eisaki, A. Damascelli, R. Yoshizaki, J.-i. Shimoyama, K. Kishio, G. D. Gu, S. Oh, A. Andrus, J. O'Donnell, J. N. Eckstein and Z.-X. Shen: Science **289** (2000) 277.
- [12] A. J. Leggett: Phys. Rev. **140** (1965) A1869.
- [13] A. J. Millis, S. M. Girvin, L. B. Ioffe and A. I. Larkin: J. Phys. Chem. Solids. **59** (1998) 1742.
- [14] T. Jujo: J. Phys. Soc. Jpn. **70** (2001) 1349.
- [15] K. Kanki and K. Yamada: J. Phys. Soc. Jpn. **66** (1997) 1103.
- [16] H. Maebashi and H. Fukuyama: J. Phys. Soc. Jpn. **66** (1997) 3577.
- [17] T. Okabe: J. Phys. Soc. Jpn. **67** (1998) 2792.
- [18] K. Yamada and K. Yosida: Prog. Theor. Phys. **76** (1986) 621.
- [19] A. A. Abrikosov, L. P. Gor'kov and I. E. Dzyaloshinskii: *Methods of Quantum Field Theory in Statistical Physics* (Pergamon, Oxford, 1965).
- [20] For example, J. R. Schrieffer: *Theory of Superconductivity* (W.A. Benjamin, New York, 1964).
- [21] P. Nozières: *Theory of Interacting Fermi Systems* (W.A. Benjamin, New York, 1964).
- [22] G. Baym and L. P. Kadanoff: Phys. Rev. **124** (1961) 287.; G. Baym: Phys. Rev. **127** (1962) 1391.
- [23] S. Koikegami, S. Fujimoto and K. Yamada: J. Phys. Soc. Jpn. **66** (1997) 1438.
- [24] V. Barzykin and D. Pines: Phys. Rev. B **52** (1995) 13585.
- [25] J. Mesot, M. R. Norman, H. Ding, M. Randeria, J. C. Campuzano, A. Paramekanti, H. M. Fretwell, A. Kaminski, T. Takeuchi, T. Yokoya, T. Sato, T. Takahashi, T. Mochiku and K. Kadowaki: Phys. Rev. Lett. **83** (1999) 840.
- [26] C. Panagopoulos, B. D. Rainford, J. R. Cooper and W. Lo, J. L. Tallon, J. W. Loram, J. Betouras, Y. S. Wang and C. W. Chu: Phys. Rev. B **60** (1999) 14617.
- [27] K. Yamada: Prog. Theor. Phys. **53** (1975) 970.
- [28] M. Imada, A. Fujimori and Y. Tokura: Rev. Mod. Phys. **70** (1998) 1039.
- [29] Y. M. Vilk and A.-M.S. Tremblay: J. Phys. I (France) **7** (1997) 1309.
- [30] G. M. Éliashberg: Sov. Phys. JETP **14** (1962) 886.

